

## SYNTHESIS OF ZnO NANOTUBES BY MPECVD

**Chang Soon Huh**

Applied Chemistry Major, Division of  
Chemical and Environmental  
Engineering, College of Engineering /  
Dong-eui University  
South Korea  
0411black@deu.ac.kr

### ABSTRACT

We have synthesized ZnO nanowires (NWs) using a microwave plasma enhanced chemical vapor deposition (MPECVD) method, which has been believed to be the most promising candidates for the synthesis of NWs due to the low temperature and the large area growth possibilities. Vertically oriented NWs were successfully synthesized by MPECVD with  $C_2H_2/H_2$  as source gases. NWs were analyzed by SEM, EDX, TEM, and XRD.

**Keywords:** Carbon nanotubes, MPECVD, Ni thin films, reaction time.

### 1. INTRODUCTION

Since the first surveillance of CNTs [1], general researches have motivated on the synthesis of CNTs with high application. Numerous synthetic methods such as arc discharge [2–4], laser vaporization [5, 6], pyrolysis [7], and plasma enhanced or thermal CVD [8–15] were engaged. Synthesis of well-aligned CNTs on a large area is necessary for one of various applications, electron emitter of field emission displays. The arc discharge and the laser vaporization techniques can produce the large amount of CNTs, but it is very difficult to control the alignment and size [4, 5]. These methods also require distillation process to dispersed pure CNTs from other particles. Many research groups have engaged the CVD method for the drive of large scaled fabrication of CNTs [8–15]. It is shown that the CVD technique can synthesize the CNTs with high purity, high yield, selective growth, and good vertical alignment. In this study, we report the vertically aligned multi walled CNTs growth on a large area of silicon oxide ( $SiO_2$ ) substrate by using MPECVD method. The surface of catalytic cobalt Nickel (Ni) film deposited on the  $SiO_2$  substrate is improved by wet hydrogen fluoride (HF) and/or subsequent hydrogen ( $H_2$ ) gas etchings. Acetylene ( $C_2H_2$ ) gas was used to produce CNTs. Despite many successful syntheses, the growth mechanism is still not completely understood. Therefore, we discuss a possible mechanism for the CNT growth.

### 2. EXPERIMENTAL AND THEORETICAL METHODS

Figure 1 shows the schematic diagram of this MPECVD experimental setup. Microwave plasma is sustained in the frequency of 2.45 GHz power supply. Microwave-excited plasmas have two appealing properties: If applied in surface-wave-sustained mode, they are especially well suited to generate large-area plasmas of high plasma density. In addition, both in surface-wave and resonator mode, they can exhibit a high degree of spatial localization. This allows to spatially separating the location of plasma generation from the location of surface processing.

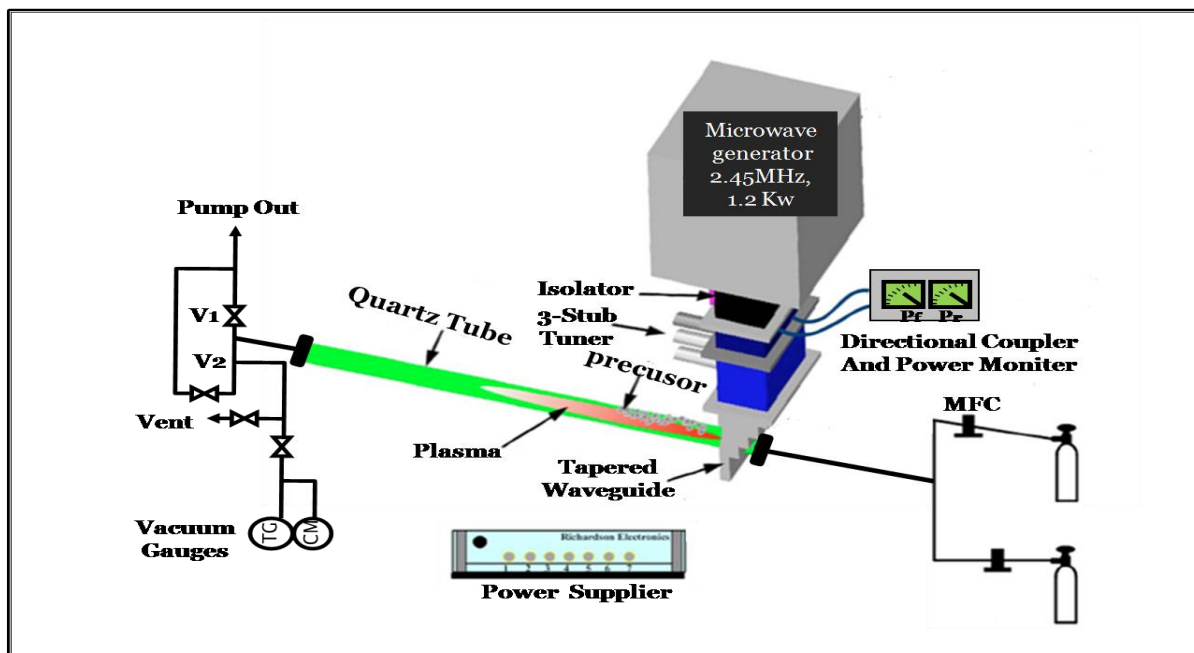


**Figure 1. Schematic diagram of Microwave Plasma Enhanced Chemical Vapor Deposition (MPECVD) system.**

\* TG: Thermocouple Gauge.  
CM: Capacitance manometer.

In trivial microwave plasmas, the electric field strength is about  $E_0 \sim 30$  V/cm, the maximum electron amplitude ( $x$ ) is less than  $10^{-3}$ , and the highest electron energy in one cycle is about 0.03 eV. In this degree, energy is insufficient of plasma sustaining so the microwave discharge in a low pressure ( $< 1$  Torr, less than DC / RF discharge) is problematic. Microwave absorption degree depends on the pressure, because it is a function of the collision frequency between electron and neutron species. In the case of 2.45 GHz microwave frequency, the effective microwave absorption has done at 5 ~ 10 Torr He pressure. The effective pressure of other gases are 0.5 ~ 10 Torr. Short wavelength (2.45 GHz corresponding to 12.24 cm) microwave plasma has local high density in a small portion and the rapid decrease of plasma density in the surrounding. The power transfer to the plasma is done through the microwave applicators - waveguide, resonance cavity, coaxial applicator. The dielectric materials (quartz, alumina and so on) separate the plasma from the microwave [Table .1].

**Table 1. Comparison of RF plasma with microwave plasma**

	RF plasma	Microwave plasma
Frequency	13.56 MHz	2.45GHz
Pressure	10 mtorr	5~50 torr
Electron Temperature (K)	$10^4 \sim 10^6$	$10^4 \sim 10^6$
Density of Plasma(*Nu./cm <sup>3</sup> )	Glow discharge $10^{10} \sim 10^{14}$	Glow discharge $10^{10} \sim 10^{14}$
Degree of Ionization (%)	0.01~0.1	1~10

\*Nu. : Number of ions per cubic centimeters

In a surface wave (SW), discharge the plasma column is sustained by the field of a guided wave that propagates along the plasma column and the dielectric containing the plasma; these media form the sole propagating and guiding structure, that is, no other wave guiding structure is required. The SW can be launched from a localized, small size exciter whose axial length can

be very small compared to the plasma column length. This length is and increasing functional of the HF power delivered to the launcher. We ignited hydrogen plasma because it particle the metal thin film and removes the amorphous carbon contamination. Panchen's law (equation 1) let us know the breakdown voltage of a gap is a non-linear function of the product of the gas pressure and the gap distance.

$$V=f(pd) \quad (1)$$

( $p$  and  $d$  are pressure and gas distance, respectively.)

The microwave source frequency is 2.45 GHz and continuous power output up to 1200 W. The circulator allows the power to go from the microwave source to the load but prevents power reflected by the load from reaching the source again, thus preventing the magnetron from overheating. The three-stub tuner is a waveguide component used to match the load impedance and minimizes the amount of reflected power, which results in the most efficient coupling of power to the load. A quartz tube, which forms the reaction chamber, passes through this cavity and reaction gasses are introduced from one end and exhausted at the other end. Temperature is measured by an R-type thermocouple, which is shielded by a ceramic tube and positioned at the outer surface of the 25.4 mm outer diameter quartz tube. For the reliable experiment, we changed the quartz tube in each experiment. System divided two zones and named as I and II (Figure 2).

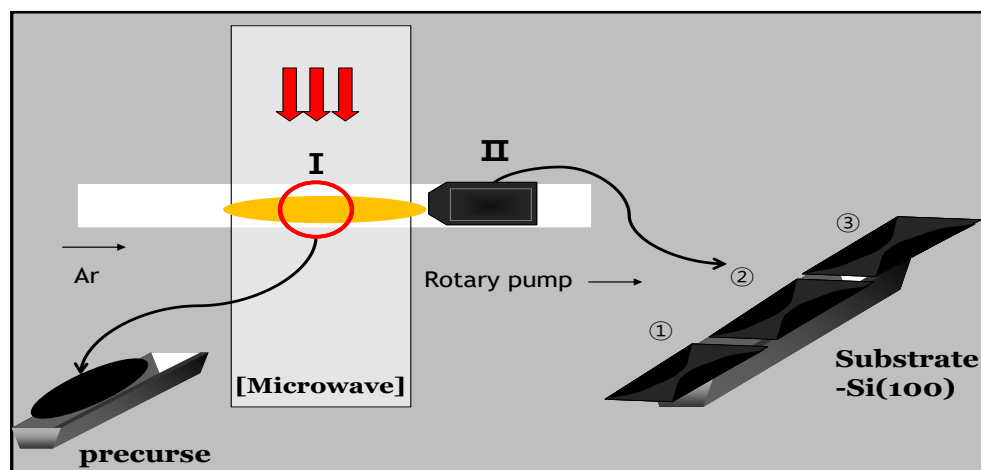


Figure 2. System divided two zones and named as “Zone 1 ” and “Zonell”.

ZnO powder was put into a quartz boat placed in the middle of the I zone. The substrate was placed in an alumina boat in the middle of II zone. Most of the experiments were done in a low vacuum circumstance (roughing pump, maximum to  $1 \times 10^{-2}$  torr). Vacuum system consists of the metering valve that applied to control the reaction pressure and the pirani gauge (Leybold, Thermovac TM20) and the capacitance manometer (MKS, Baratron type 626A). The carrier-gas controlled by MFCs (MKS, type 1179) and exhaust gas flew into the LN2 trap for protecting the rotary pump.

### 3. RESULTS

We have grown ZnO nanotubes using a MPECVD method, which has been believed to be the most promising candidates for the synthesis of NWs due to the low temperature and the large area growth possibilities. Wool-like ZnO nanotubes were successfully synthesized by

MPECVD with  $C_2H_2/H_2$  as source gases. Additionally, non-catalytic method used in an experiment on the growth of ZnO nanotubes on  $SiO_2/Si$  wafer. The experimental scheme was shown in Figure 1. Zinc Oxide powder was put into a quartz boat placed in the middle of the I zone. The  $SiO_2/Si$  substrate was placed in an alumina boat in the middle of II zone. As protective gas and carrier gas, pure Ar (flow rate 100 sccm). The Ar plasma ignited at 0.1 Torr with flow Ar 40 sccm, 400 W there after  $H_2$  80sccm flow into the chamber and made hydrogen plasma environment and acetylene ( $C_2H_2$ ) 3 sccm flew the chamber about 10 min at 10 torr to make ZnO nanotubes synthesis condition. The temperature of the microwave plasma was estimated about 1000 °C. After reaction for 10 min,  $H_2$  flow was stopped and black ZnO nanotubes product around the inner wall of the quartz tube could be observed. In microwave plasma system, ZnO nanotubes were grown from ZnO powders under an  $H_2$  atmosphere inside the quartz tube reactor. Because no catalyst is used in the system. The ZnO nanowire growth should be based on a self-catalytic vapor-liquid-solid mechanism. These nanowires act as hard templates to determine the nanowire forms. Low concentration  $O_2$ , diluted by insert gas Ar, is introduced into the reaction chamber (quartz tube) for particle oxidation of ZnO nanowires. After the experiment, white wool-like ZnO nanotubes were obtained in the collector, and the morphology and structure of the synthesized products are shown in SEM images (Figure 3).

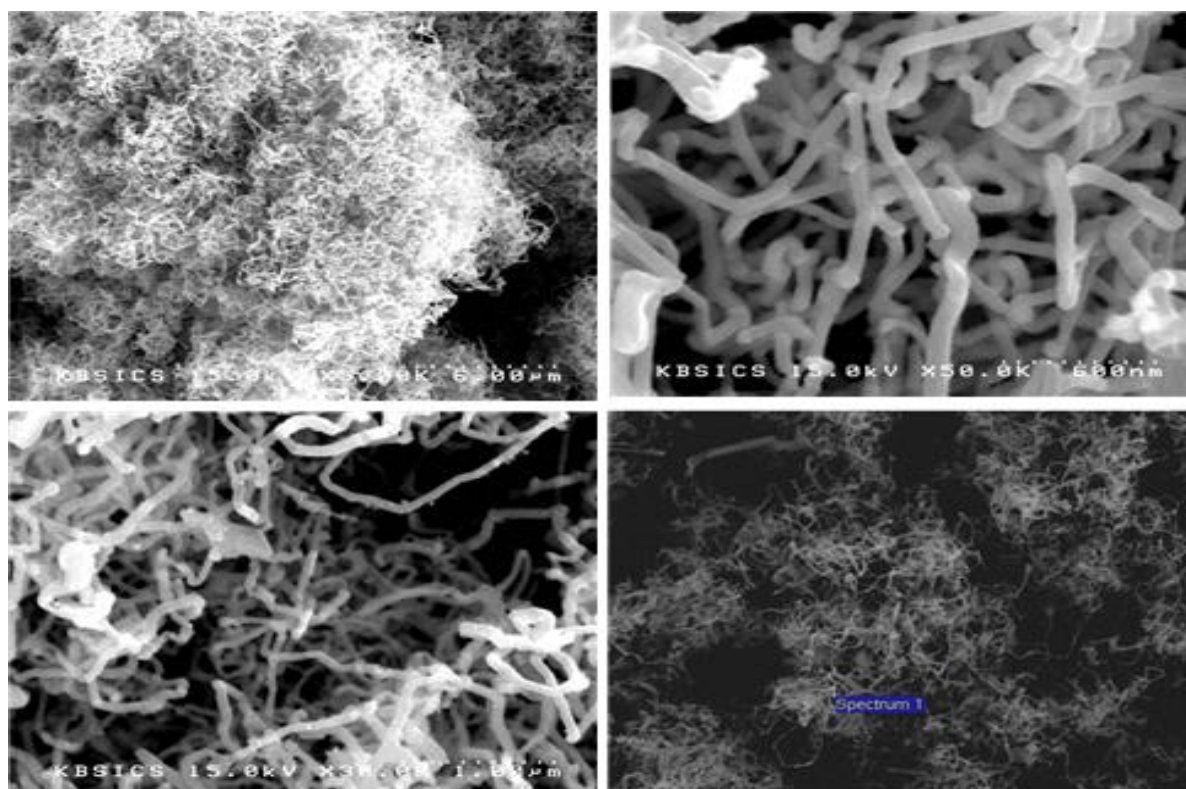


**Figure 3. SEM images of ZnO nanotubes deposited on  $SiO_2/Si$  substrate.**

A transmission electron microscopy (TEM, JEM 2011, accelerating voltage range 80~200 kV) images of the products shows each nanostructure is assembled by nanowires, with diameters ranging from 30 ~ 40 nm. From TEM image, we know that the nanostructures are ZnO nanotubes and many curved NWs seem from the plasma impact (Figure 4).



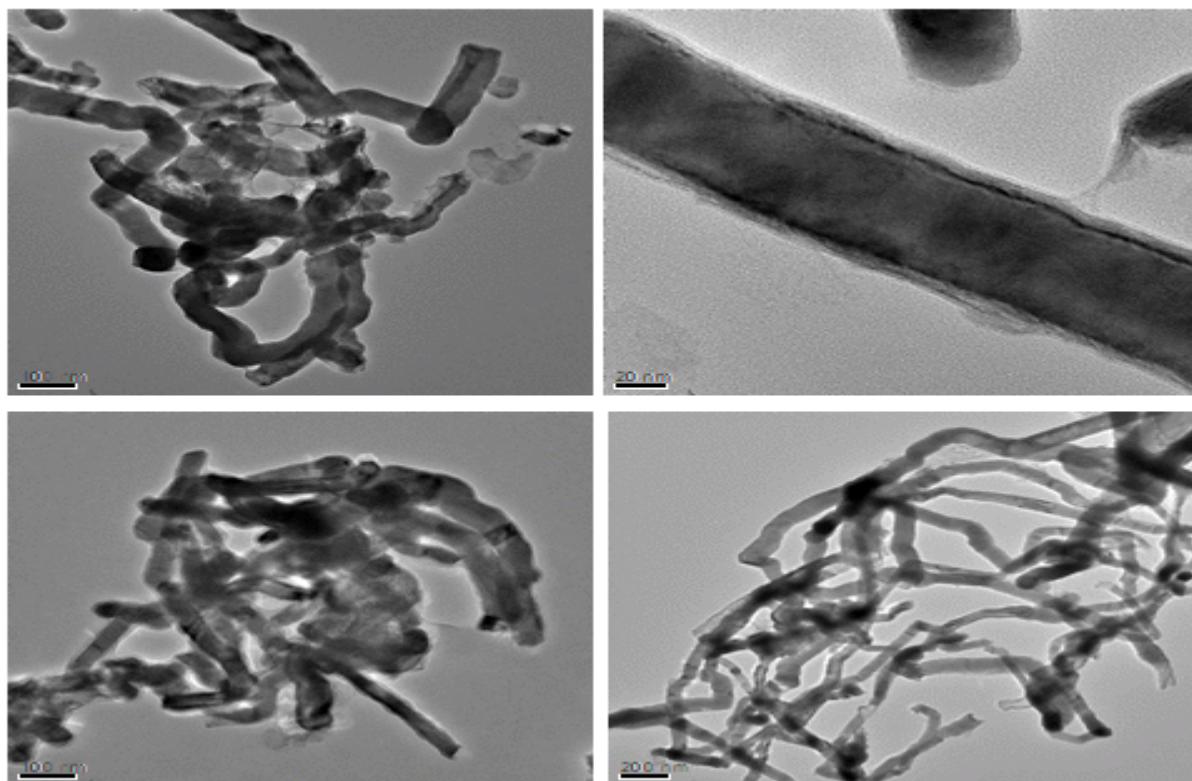
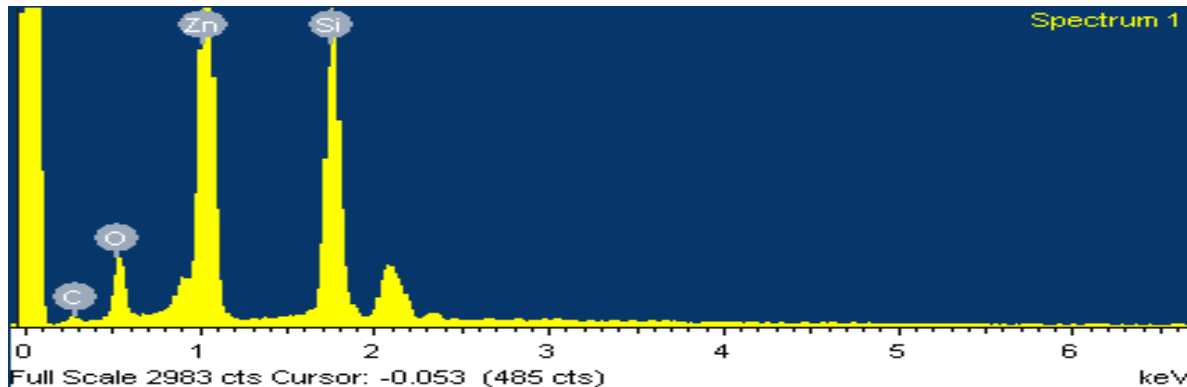


**Figure 4. TEM images of ZnO nanotubes deposited on SiO<sub>2</sub>/Si substrate.**  
Energy-dispersive spectroscopy (EDS) identifies that the composition of the NWs is Zn, O



Element	Weight%	Atomic%
C K	6.63	17.93
O K	11.83	24.02
Si K	26.59	30.75
Zn L	54.95	27.30
Totals	100.00	

(Figure 5). The Zn content is about 27.30 atom percentage.

**Figure 5. EDX spectrums of the face on SiO<sub>2</sub>/Si wafer (Spectrum 1 in Figure 3)**

Figure 6 shows the typical x-ray diffraction spectra (XRD, 1.2kW Cu K $\alpha$ ,  $\lambda=1.54\text{\AA}$ ) of these ZnO nanotubes (JCPDS card No. 800075). These spectra can be indexed for diffraction from the (1 0 0), (0 0 2), (1 0 1), (1 0 2), and (1 0 3) planes of wurtzite crystals, which are

corresponding to ZnO.

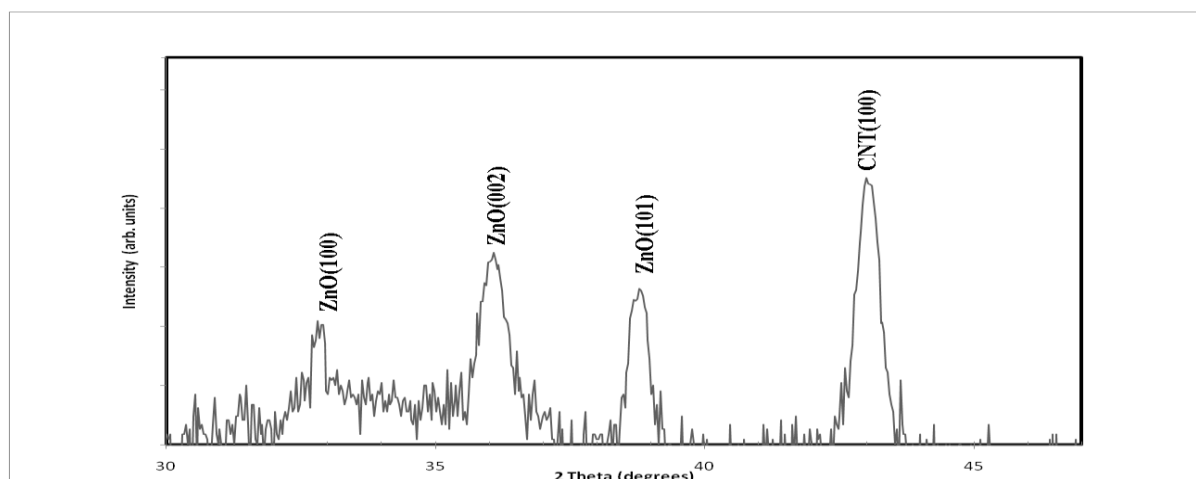


Figure 6. XRD patterns of ZnO nanowire deposited on SiO<sub>2</sub>/Si substrate.

#### 4. DISCUSSION

Many fractures of multiwall CNTs seem from the plasma impact. Two different growth modes can be suggested based on the interaction of the catalyst with its support as described by Baker [19]. The interaction of the catalyst with the support can be characterized by its contact angle at the growth temperature, analogous to “hydrophobic” (weak interaction) and “hydrophilic” (strong interaction) surfaces. Thus, the surface interaction between the catalyst and its support is an important consideration which dictates the growth mode (Figure 7). The tip growth model was suggested to explain the SEM images of CNTs (Figure 4). Also, we can identify the structure of CNTs by TEM image analysis with Figure 5. The hollow tip with any Ni catalytic particles, as seen from Figure 5, is inconsistent with the tip growth model. When the MPECVD method was used for the CNT synthesis, the catalytic particles usually remain at the tip of CNTs, which was justified by the tip growth model. Therefore, in order to explain the hollow tip of CNTs as well as the bamboo structure, the tip growth model would be rather suitable. In the growth reaction of CNTs, the diffusion of carbon in the catalyst metal has been believed to be the rate-determining step. The growth rate of CNTs can be described by an Arrhenius equation that the activation energy is the diffusion energy of carbon in the metal. Support for this model comes from experiments on the kinetics of growth of CNTs on the  $\gamma$ -Ni metal from acetylene at 1000 °C, yielding the activation energy of 142 kJ mol<sup>-1</sup>, which is close to the activation energy for diffusion, 148 kJ mol<sup>-1</sup> [20, 21]. So we concluded that the bamboo-typed MWNTs growth follows the tip-growth mode. It seems to be the high interaction between nickel thin film and titanium nitride buffer layer.

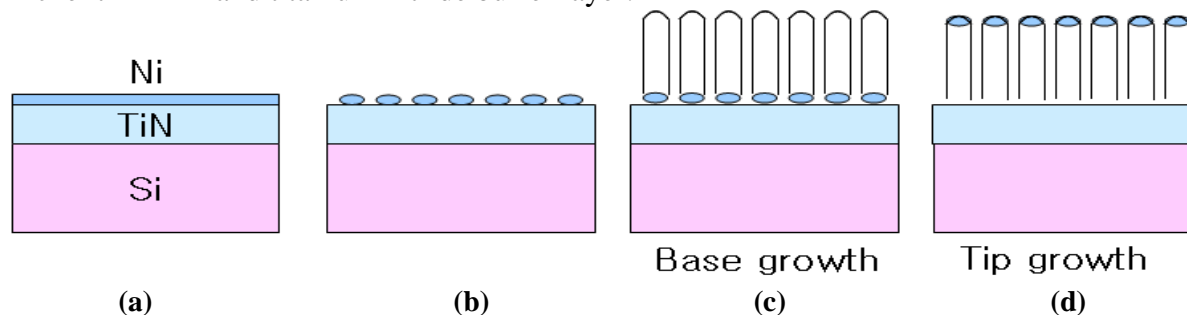


Figure 7. Growth mode of CNTs. The multilayer thin film, Ni: 20 nm TiN: 100 nm (a) after the annealing (b), base growth mode (c) and tip growth mode (d).

## 5. CONCLUSIONS

We have grown the vertically well aligned bamboo type multi walled CNTs on a large area of Ni deposited SiO<sub>2</sub> substrates using the MPECVD method. The diameter of CNTs is 30 nm and the length is about 60  $\mu$ m length. The multi walled CNTs have the hollow tip and the bamboo structure that the hollow compartments are separated with the graphite layers. The multi walls are in good crystalline phase. The tip growth mechanism is suitable for the CNTs grown by MPECVD. We suggest that surface and bulk diffusions of carbons play an important role in determining the structure of CNTs. The vertically aligned multi walled CNTs grown on the Ni deposited substrate can be applicable to the many fields.

## ACKNOWLEDGEMENTS

This research did not receive any specific grant from funding agencies in the public, commercial, or not-for-profit sectors.

## REFERENCES

- [1] S. Iijima. (1991) Helical microtubules of graphitic carbon. *Nature*, 354, 56-58.
- [2] S. Iijima, T. Ichihashi. (1993) Single-shell carbon nanotubes of 1-nm diameter. *Nature*, 363, 603.
- [3] D.S. Bethune, C.H. Kiang, M.S. deVries, G. Gorman, R. Savoy, J. Vazquez, R. Beyers. (1993) Cobalt-catalysed growth of carbon nanotubes with single-atomic-layer walls. *Nature*, 363, 605.
- [4] C. Journet, W.K. Maser, P. Bernier, A. Loiseau, M. Lamy de la Chapelle, S. Lefrant, P. Deniard, R. Lee, J.E. Fischer. (1997) Large-scale production of single-walled carbon nanotubes by the electric-arc technique. *Nature*, 388, 756.
- [5] A. Thess, R. Lee, P. Nikolaev, H. Dai, P. Petit, J. Robert, C. Xu, Y.H. Lee, S.G. Kim, D.T. Colbert, G. Scuseria, D. Tomanek, J.E. Fisher, R.E. Smalley. (1996) Crystalline Ropes of Metallic Carbon Nanotubes. *Science*, 273, 483.
- [6] M. Yudasaka, R. Yamada, N. Sensui, T. Wilkins, T. Ichi-hashii, S. Iijima. (1999) Estimation of the Charge Injection Barrier at a Metal/Organic Semiconductor Interface Based on Accumulated Charge Measurement: The Effect of Offset Bias Voltages. *J. Phys. Chem. B*, 103, 6224.
- [7] M. Terrones, N. Grobert, J. Olivares, J.P. Zhang, H. Terrones, K. Kordatos, W.K. Hsu, J.P. Hare, P.D. Townsend, K. Prassides, A.K. Cheetham, H.W. Kroto, D.R.M. Walton, (1997) Efficient route to large arrays of CN<sub>x</sub> nanofibers by pyrolysis of ferrocene/melamine mixtures. *Nature*, 388, 52.
- [8] Z.F. Ren, Z.P. Huang, J.W. Xu, J.H. Wang, P. Bush, M.P. Siegal, P.N. Provencio. (1998) Synthesis of large arrays of well-aligned carbon nanotubes on glass. *Science*, 282, 1105.
- [9] S.L. Sung, S.H. Tsai, C.H. Tseng, F.K. Chiang, X.W. Liu, H.C. Shih. (1999) Bias-enhanced nucleation and growth of the aligned carbon nanotubes with open ends under microwave plasma synthesis. *Appl. Phys. Lett*, 74, 197.
- [10] W.Z. Li, S.S. Xie, L.X. Qian, B.H. Chang, B.S. Zou, W.Y. Zhou, R.A. Zhao, G. Wang. (1996) Large-Scale Synthesis of Aligned Carbon Nanotubes. *Science*, 274, 1701.
- [11] S. Fan, M.G. Chapline, N.R. Franklin, T.W. Tomblor, A.M. Casell, H. Dai. (1999) Self-oriented regular arrays of carbon nanotubes and their field emission properties. *Science*, 283, 512-514.

- [12] C.J. Lee, D.W. Kim, T.J. Lee, Y.C. Choi, Y.S. Park, W.S. Kim, Y.H. Lee, W.B. Choi, N.S. Lee, K.S. Park, J.M. Kim. (1999) One-step formation of aligned carbon nanotube field emitters at 400°C. *Chem. Phys. Lett*, 312, 461.
- [13] C.J. Lee, J. Park, S.Y. Kang, J.H. Lee. (2002) Uniform field emission from aligned carbon nanotubes prepared by CO disproportionation. *Journal of Applied Physics*, 92, 7519.
- [14] C.J. Lee, D.W. Kim, T.J. Lee, Y.C. Choi, Y.S. Park, W.S. Kim, Y.H. Lee, W.B. Choi, N.S. Lee, J.M. Kim, Y.G. Choi, S.C. Yu. (1999) Fully sealed, high-brightness carbon-nanotube field-emission display. *Appl. Phys. Lett*, 75, 1721.
- [15] C.J. Lee, J. Park, S.Y. Kang, J.H. Lee, C.J. Lee, J.H. You. (2002) Triode field emitter with a gated planar carbon-nanoparticle cathode. *Appl. Phys. Lett*, 81, 358.
- [16] Cheol Jin Lee a.), Jeunghee Park, Seung Youl Kang, Jin Ho Lee. (2000) Growth and field electron emission of vertically aligned multiwalled carbon nanotubes. *Chemical Physics Letters*, 326, 175–180.
- [17] P.Taylor. (1998), Ostwald ripening in emulsions. *Advances in Colloid and Interface Science*, 75, 2, 16, 107-163.
- [18] D. W. Hess et al. (2005) Aligned Carbon Nanotube Stacks by Water-Assisted Selective Etching. *Nano Lett*, , 5, 2641-2645.
- [19] R. T. K. Baker. (1989) Catalytic growth of carbon filaments. *Carbon*, 27, 315.
- [20] R.T.K. Baker, J.J. Chludzinski, C.R.F. Lund. (1987) *Extended Abstracts of the 18th Biennial Conference on Carbon, Worster Polytechnic Institute*, 155.
- [21] C.J. Smithellsin: E.A. Brandes, G.B. Brook Eds., Smithells Ž. (1992) *Metals Reference Book*, 7th edn., Butterworth-Heinemann,